

Wetness and Color from A Single Multispectral Image

Mihoko Shimano[†] Hiroki Okawa[‡] Yuta Asano[‡] Ryoma Bise[†] Ko Nishino^{†*} Imari Sato[†]

[†]National Institute of Informatics [‡]Tokyo Institute of Technology ^{*}Drexel University
 {miho,bise-r,imarik}@nii.ac.jp {okawa.h.ac,asano.y.ac}@m.titech.ac.jp kon@drexel.edu

Abstract

Visual recognition of wet surfaces and their degrees of wetness is important for many computer vision applications. It can inform slippery spots on a road to autonomous vehicles, muddy areas of a trail to humanoid robots, and the freshness of groceries to us. In the past, monochromatic appearance change, the fact that surfaces darken when wet, has been modeled to recognize wet surfaces. In this paper, we show that color change, particularly in its spectral behavior, carries rich information about a wet surface. We derive an analytical spectral appearance model of wet surfaces that expresses the characteristic spectral sharpening due to multiple scattering and absorption in the surface. We derive a novel method for estimating key parameters of this spectral appearance model, which enables the recovery of the original surface color and the degree of wetness from a single observation. Applied to a multispectral image, the method estimates the spatial map of wetness together with the dry spectral distribution of the surface. To our knowledge, this work is the first to model and leverage the spectral characteristics of wet surfaces to revert its appearance. We conduct comprehensive experimental validation with a number of wet real surfaces. The results demonstrate the accuracy of our model and the effectiveness of our method for surface wetness and color estimation.

1. Introduction

Recognition of surface conditions of scene constituents, not just what they are (object recognition) and where they are (place recognition) but whether they are, for instance, clean, smooth, rusty, or soft, is vital for computer vision to succeed in the real world. Wetness is one of the key surface conditions that is critical to robustly recognize in computer vision applications. Water or other liquids absorbed by the surface cause muddy trails that humanoid robots may have to carefully walk over, slippery roads after rain for autonomous vehicles to brake earlier, and fruits to maintain their freshness for us to consume. The degree of wetness

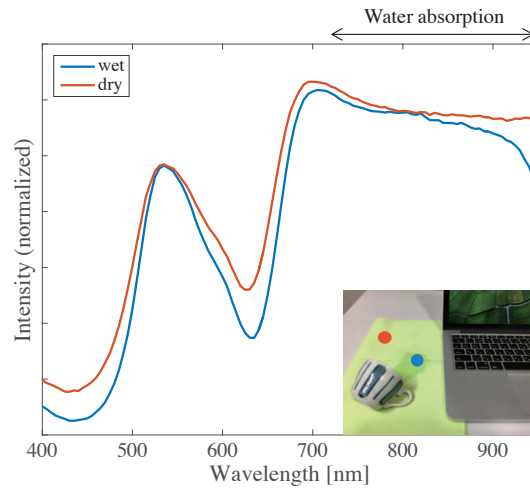


Figure 1: Example spectral distributions of dry and wet surface points (red and blue curves, respectively). The wet spectral distribution shows characteristic darkening (decrease in magnitude) and spectral sharpening (narrowing of distribution, i.e., contrast increase). The spectral energy is normalized for better visualization; the actual magnitude is significantly higher than that of the wet surface across the spectrum. We derive a novel spectral appearance model that accurately encodes both of these characteristics of wet surfaces and use it to estimate wetness and color from a single multispectral image.

directly reflects the desirable or undesirable condition of the surface: the more the muddier and the fresher. Can we estimate the wetness of a surface just from its looks? In this paper, we derive a rigorous spectral appearance model for water-wet surfaces. Our model and method for surface wetness and color recovery, however, can be applied to any liquid if we know its spectral behavior.

Making a surface wet causes characteristic appearance change. As shown in Figure 1, there are two fundamental components to this appearance change. The first is the decreased intensity across the spectrum, whose magnitude is proportional to the degree of wetness. This monochromatic characteristic of wet surface appearance has been modeled

and used for recognition and image synthesis in the past. For the special case when a thin film of water is present on the surface, Angstrom [1] showed that the probability of light being absorbed by the surface due to internal reflection at the film-air interface increases and leads to darkening of the surface appearance. Lekner and Dorf [9] derived a more accurate model of this phenomenon, which was used to recognize wet surfaces and estimate its dry appearance by controlling the brightness [11, 19].

The main cause of the darkening is, however, due to the water absorbed by the surface itself. Twomey et al. [16] showed that light scattering in the surface becomes more forward-centered when the surface becomes wet, leading to the darkening, which agrees with the spectral model we derive. Jensen et al. [8] combined this model with that of Lekner and Dorf to render wet surfaces. Data-driven models based on images of surfaces with varying degrees of dryness have also been introduced for image synthesis [10, 5, 14, 20]. These models, however, do not explicitly relate the degree of surface wetness to its appearance.

Perhaps less known is the second characteristic appearance change of wet surfaces: the effect of water (liquid) absorbed by the surface on its spectral behavior. As shown in Figure 1, the spectral distribution of a wet surface region becomes sharper than that of a dry region with the same surface color. As we show in this paper, this is due to the complex interplay of light absorption and multiple scattering inside the surface. Although this important spectral characteristic of wet surfaces has been empirically studied for image synthesis [10], to our knowledge, it has not been rigorously modeled in the past.

In this paper, we derive a comprehensive spectral appearance model of wet surfaces. We specifically focus on the general appearance change induced by liquid absorbed in the surface itself. Our model explains both the monochromatic darkening and spectral sharpening of wet surfaces. It also rigorously relates the degree of surface wetness to its appearance change. Collectively, the model enables the recovery of the degree of wetness and the original (dry) surface color from a single observation. The model is derived based on two key ideas for describing light behavior in wet surfaces. The first is to represent the scattering anisotropy with a linear combination of its distributions when the surface is completely dry and completely wet. This enables us to relate the degree of wetness to the shape of anisotropic scattering with a single parameter. The second is to express the light absorption rate for light scattering in the surface with a single parameter by interpreting the light interaction as a stochastic walk through wet and dry areas in the surface. We assume that the overall optical path length during multiple scattering can be separated into paths in wet and dry areas, and define the degree of wetness as the proportion of wet paths in the overall optical path. These two key

assumptions enable us to express the complex appearance of surfaces with arbitrary degrees of wetness with a simple bilinear equation. The bilinear model consists of a Hadamard product of a matrix expressing the spectral surface color and a Vandermonde matrix encoding light absorption by the liquid induced by multiple scattering, and a matrix representing the degree of wetness of the surface.

Our model lends itself to a simple yet powerful method for recovering the surface wetness and original color from a single observation. We assume that the spectral distribution of absorption by the liquid is known or can be measured a priori [2]. We show that we can recover a spatial map of surface wetness and the original (dry) spectral distribution from a single multispectral image. The recovered wetness is absolute if there are completely dry and completely wet points of the same material in the image. It becomes relative to the driest or wettest point if neither are present. We also demonstrate that we can recover the underlying texture and spatial wetness of a wet textured surface.

We conduct an extensive quantitative evaluation of the method using various real-world surfaces. The experimental results validate the accuracy of our model and show that we can accurately recover the surface wetness and color from a single multispectral image. These results demonstrate a promising first step for recognizing and estimating surface conditions from appearance.

2. A Spectral Model of Multiple Scattering

In this section, we derive an analytical spectral appearance model of wet surfaces. We first derive a spectral appearance model for dry surfaces and extend it to wet surfaces. Scattering is the key radiometric behavior in a wet surface. Although light scattering in participating media has been studied in the past [3, 13, 6, 12] and applied to critical applications including remote sensing [4, 18, 17] and medical imaging [8, 15], its spectral behavior in wet surfaces still remains to be addressed.

2.1. Light Scattering in Dry Surfaces

Surfaces consist of particles interwoven with air or other medium that cause scattering and absorption every time a light ray hits them. These radiometric events determine the color and brightness of the surface. We start our derivation with the simple case of single scattering at a certain wavelength. Let us denote the irradiance received at a surface point with I_0 . According to a widely adopted single scattering model [13], the intensity of light after single scattering can be computed as the product of the incident irradiance I_0 , the phase function that approximates the scattered light

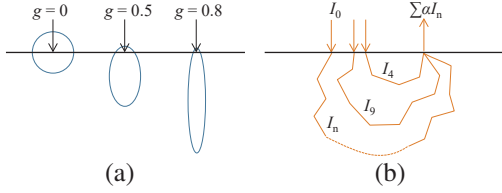


Figure 2: (a) The relation between the scattering parameter g and the shape of the scattering distribution. (b) Different light paths with varying degrees of scattering inside the surface collectively radiate from the same surface point.

distribution, and the light absorption in the surface:

$$\begin{aligned} I_1(g, \omega, u, r_1) &= I_0 p(g, \omega) e^{-ur_1} \\ p(g, \omega) &= \sum_{l=0}^{\infty} \frac{(2l+1)}{4\pi} g^l P_l(\omega \cdot \omega_0), \end{aligned} \quad (1)$$

where $p(g, \omega)$ is the empirical Henyey-Greenstein phase function, $g(-1 \leq g \leq 1)$ is the scattering anisotropy parameter that encodes the shape of the scattering distribution, ω is the viewing direction, and P_l is the Legendre Polynomial. As shown in Figure 2(a), the shape of the scattering distribution becomes isotropic when $g = 0$, and it becomes forward scattering when g is near 1, and backward scattering when g is near -1. The third term describes the amount of light absorbed by the material when it travels from the first scattering point to the second, which is computed using the absorption coefficient u and the path length r_1 , where the subscript denotes the number of scattering.

Similarly, light leaving from a surface after experiencing n times of scattering can be expressed with the product of the incident irradiance, the averaged phase function across the first to the n -th ones, and the light absorption

Now, let us derive the radiance (intensity) of a dry surface by accounting for multiple scattering. As shown in Figure 2(b), a surface point will be radiating a collection of light rays that experience varying degrees of multiple scattering. We assume that scattering particles of the surface are uniformly distributed, and the scattering parameter g_d and the absorption coefficient u of a dry surface is spatially uniform (i.e., we focus on a surface region of identical material). We also implicitly assume that the surface is flat and the incident lighting is angularly uniform (e.g., ambient environmental light). Under these assumptions that hold for general flat surface regions of the same color, the intensity of a surface can be expressed as a weighted sum over n -times scattered light of the surface irradiance I_0 :

$$\begin{aligned} I_d(g_d, \omega, u, r_n) &= \sum_n \alpha(g_d, n) I_n(g_d, \omega, u, r_n) \\ &= I_0 \sum_n \alpha(g_d, n) p^{[n]}(g_d, \omega) e^{-ur_n} \\ &\approx I_0 \sum_n \alpha(g_d, n) p^{[n]}(g_d, \omega) e^{-unr_0}, \end{aligned} \quad (2)$$

where the weight function $\alpha(g_d, n)$ is the ratio of light that experiences n -times scattering before reaching the surface point of interest and $p^{[n]}$ is the n -times convolution of the phase function. We assume that the mean light path length r_0 is the same regardless of the number of scattering n , which leads to the total path length $r_n \approx nr_0$.

2.2. Light Scattering in Wet Surfaces

Let us now turn our attention to the case when the surface becomes wet. We can consider wet surfaces as having liquid replacing the air between scattering particles. The interwoven liquid affects the overall shape of the scattering distribution and introduces additional absorption during scattering. The degree of wetness defines how much liquid was absorbed into the surface. In this section, we model how the intensity of a surface point changes as a function of the degree of wetness.

We first consider the extreme case, in contrast to a completely dry surface, when the liquid fills all areas between scattering particles. We refer to this completely wet condition as “saturated.” We assume that light absorption by the surface between successive scattering can be determined by the product of absorption in the original dry surface and that of the liquid itself. This is a safe assumption to make as long as the surface material and the liquid absorbed by the surface are spatially exclusive (i.e., the material is not soluble in the liquid). The intensity of a saturated surface point can then be expressed as

$$\begin{aligned} I_s(g_s, \omega, u, v, r_0) &= I_0 \sum_n \tau_n(g_s, \omega) a(u, r_0)^n b(v, r_0)^n \\ \tau_n(g_s, \omega) &= \alpha(g_s, n) p^{[n]}(g_s, \omega) \\ a(u, r_0) &= e^{-ur_0} \\ b(v, r_0) &= e^{-vr_0}, \end{aligned} \quad (3)$$

where g_s is the scattering parameter of the saturated surface, and v is the absorption coefficient of the liquid. g_s is usually larger than g_d since the scattering parameter of liquid is generally higher than that of air.

Next, let us consider the general case of wet surfaces: liquid partially filling the surface. Without loss of generality, instead of considering partial replacement of air between scattering particles with liquid, we interpret wet surfaces as consisting of saturated and dry areas co-existing under the surface with a ratio proportional to the degree of wetness. With this definition of wet surfaces, the overall light path length during multiple scattering can be separated into saturated paths and dry paths. The degree of the wetness γ is defined as the ratio of wet area in the overall light path, where γ is 0 if the surface is completely dry, and γ is 1 if it is completely wet (i.e., saturated). The scattering

parameter of wet surfaces g_w then becomes

$$\begin{aligned} p^{[n]}(g_w, \omega) &= p^{[(1-\gamma)n]}(g_d, \omega)p^{[\gamma n]}(g_s, \omega) \\ &= \sum_{l=0}^{\infty} \frac{(2l+1)}{4\pi} g_d^{(1-\gamma)nl} g_s^{\gamma nl} P_l(\omega \cdot \omega_0) \\ &= p^{[n]}(g_d^{(1-\gamma)} g_s^\gamma, \omega) \end{aligned} \quad (4)$$

$$g_w = g_d^{(1-\gamma)} g_s^\gamma. \quad (5)$$

The absorption in wet surfaces with a degree of wetness γ can be written as $a(u, r_0)b(v, r_0)^\gamma$. The intensity of wet surfaces is derived by substituting this into Equation 3

$$\begin{aligned} I_w(g_d, g_s, \omega, u, v, \gamma, r_0) &= I_0 \sum_n \alpha(g_w, n) p^{[n]}(g_w, \omega) a(u, r_0)^n b(v, r_0)^{\gamma n} \\ &= I_0 \sum_n \tau_n(g_w, \omega) a(u, r_0)^n b(v, r_0)^{\gamma n}. \end{aligned} \quad (6)$$

When the degree of wetness takes on a large value (i.e., when the surface becomes more wet), the scattering parameter g_w also becomes large from Equation 5. This makes the scattering more concentrated in the forward direction. As a result, the overall light path length of multiple scattering before it reaches the surface interface back into the air becomes longer. Intuitively, this means the incident light will penetrate deeper before it comes back. In other words, the surface becomes optically thicker. This increases the total amount of absorption during multiple scattering which explains darkening of wet surfaces.

2.3. Spectral Scattering in Wet Surfaces

Let us now model the spectral behavior of light in wet surfaces by extending the monochromatic model we just derived. We will visit each of the properties of the multiple scattering model that are wavelength dependent. We assume Mie scattering which is insensitive to wavelength differences [7]. The scattering parameter g (g_d for dry, g_s for saturate, and g_w for general wet surfaces) is thus a constant for any wavelength. Since light absorption usually varies depending on the wavelength, we denote the absorption coefficient with $u(\lambda_k)$, $v(\lambda_k)$, where λ_k is the k -th wavelength we measure with a spectrometer or multispectral camera ($k = \{1, \dots, K\}$). The weight function α and the phase function p do not depend on wavelength. With these notations, the spectral appearance model of wet surfaces can be written as

$$\begin{aligned} I(g_d, g_s, u(\lambda_k), v(\lambda_k), \gamma) &= I_0 \sum_n \tau_n(g_w, \omega) a(u(\lambda_k), r_0)^n b(v(\lambda_k), r_0)^{\gamma n}. \end{aligned} \quad (7)$$

The conditions ‘dry’ and ‘saturated’ are the two extreme cases of this model with $\gamma = 0$ and $\gamma = 1$, respectively.

We can simplify notations by assuming that the incident light is a pre-calibrated white light source and, as a result, the incident illumination I_0 can be normalized to 1. The

phase function $p^{[n]}(g, \omega)$ can be rewritten as $p(g^{[n]}, \omega)$ from its definition (Equation 1). Since the incident light is angularly uniform, we may consider ω to be constant:

$$\begin{aligned} \tau_n(g) &= \alpha(g, n) p^{[n]}(g) = \alpha(g, n) p(g^n) \\ a_k &= e^{-u(\lambda_k)r_0} \\ b_k &= e^{-v(\lambda_k)r_0}. \end{aligned}$$

The spectral appearance model of wet surfaces can be expressed in a concise matrix form

$$\begin{aligned} \mathbf{W} &= (\mathbf{A} \circ \mathbf{B})\mathbf{T} \quad (8) \\ \mathbf{W} &= [w_1, \dots, w_K, \dots, w_N]^T \\ \mathbf{A} &= \begin{bmatrix} (a_1)^1 & (a_1)^2 & \dots & (a_1)^N \\ (a_2)^1 & (a_2)^2 & \dots & (a_2)^N \\ \vdots & \vdots & (a_k)^n & \vdots \\ (a_K)^1 & (a_K)^2 & \dots & (a_K)^N \end{bmatrix} \\ \mathbf{B} &= \begin{bmatrix} (b_1)^\gamma & (b_1)^{2\gamma} & \dots & (b_1)^{N\gamma} \\ (b_2)^\gamma & (b_2)^2 & \dots & (b_2)^{N\gamma} \\ \vdots & \vdots & (b_k)^{n\gamma} & \vdots \\ (b_K)^\gamma & (b_K)^{2\gamma} & \dots & (b_K)^{N\gamma} \end{bmatrix} \\ \mathbf{T} &= [\tau_1, \dots, \tau_K, \dots, \tau_N]^T, \end{aligned}$$

where w_k is the intensity of the wet surface for the k -th wavelength λ_k , and N is the maximum number of multiple scattering we consider. The operator \circ denotes Hadamard product. Matrix \mathbf{A} encodes the spectral distribution of the surface, matrix \mathbf{B} represents the absorption by up to N -th multiple scattering, and \mathbf{T} expresses the transmission by the phase function as a function of wetness. Matrix \mathbf{B} is a Vandermonde matrix reflecting the fact that the intensity of a wet surface point becomes a polynomial evaluation of multiple scattering as seen in Equation 7.

We can extend this spectral appearance model for a wet surface point to express a wet surface spanning multiple pixels ($m = \{1, 2, \dots, M\}$)

$$\begin{aligned} \mathcal{W} &= (\mathcal{A} \circ \mathcal{B}) * \mathcal{T} = \mathcal{C} * \mathcal{T} \quad (9) \\ \mathcal{C} &= (\mathcal{A} \circ \mathcal{B}), \end{aligned}$$

where \mathcal{W} is a $K \times M$ second-order tensor, \mathcal{T} is a $N \times M$ second-order tensor, and \mathcal{A}, \mathcal{B} , and \mathcal{C} are $K \times N \times M$ third-order tensors. The operator $*$ denotes that when $\mathcal{W} = \mathcal{C} * \mathcal{T}$, the m -th first-order vector \mathcal{W}_m of \mathcal{W} is computed by the product of the m -th matrix \mathcal{C}_m and vector \mathcal{T}_m for each m individually. For instance, the element $\mathcal{W}(k, m)$ can be computed by $\sum_n \mathcal{C}(k, n, m) \mathcal{T}(n, m)$.

3. Surface Wetness and Color Recovery

Based on the newly derived spectral appearance model, we establish a method for simultaneously estimating the degree of wetness and the original (dry) spectral distribution of a surface from a single multispectral observation.

3.1. Problem Setup

As derived in Equation 7, the interaction of light scattering and absorption by the liquid and surface is bilinear. The inversion of this model is thus inherently ill-posed. To enable robust estimation of its parameters, we make additional but realistic assumptions. First, we assume that the type of liquid is known so that the multispectral absorption coefficients of the liquid $\mathbf{v} = [v(\lambda_1), \dots, v(\lambda_K)]$ is known or can be measured beforehand. Second, we assume that we can specify a region of the surface with the same material (i.e., same dry color). If the image is of a homogeneous material, we can directly apply our method on the entire image. Third, we assume that we can identify saturated and dry pixels in each homogeneous surface region. If neither are available, the degree of wetness we estimate will become relative to the “saturated” and “dry” pixels that we automatically assign. For our experiments, we simply use the darkest and brightest points as the saturated and dry points, respectively. The scattering parameter can also be considered as inherently relative. We empirically found that, unless we use a large value close to 1 for g_d , the optimization is not sensitive to the selection of g_d . From this observation, we set $g_d = 0.6$ for all experiments.

We determine the weight function $\alpha(g, n)$ based on Monte Carlo simulation. We first simulate multiple scattering for each g in Equation 1 for perpendicular incident light. Then we compute the ratio of light that returns to the surface interface after n -times scattering. We fit a log-normal function to the simulation results and use it in the optimization.

Given \mathcal{W} , g_d , and \mathbf{v} , where \mathcal{W} is multiplied by the camera gain β in the optimization, we estimate the degrees of wetness for M pixels $\gamma = [\gamma_1, \dots, \gamma_M]$, the absorption coefficients of the dry surface $\mathbf{u} = [u(\lambda_1), \dots, u(\lambda_K)]$, the mean light path length r_0 , and the scattering parameter g_s

$$\begin{aligned} & \min_{\mathbf{u}, \gamma, r_0, \beta, g_s} \|\beta \mathcal{W} - (\mathcal{A}(\mathbf{u}, r_0) \circ \mathcal{B}(\mathbf{v}, r_0)) * \mathcal{T}(g_d, g_s, \gamma)\|^2 \\ & \text{s.t., } 0 \leq u(\lambda_k) \quad (k = 1, \dots, K) \\ & \quad g_d < g_s < 1 \\ & \quad 0 < r_0, \quad 0 < \beta \\ & \quad 0 \leq \gamma_m \leq 1 \quad (m = 1, \dots, M), \end{aligned} \quad (10)$$

in which, if we estimate \mathbf{u} , γ , r_0 , β , and g_s , the tensors \mathcal{A} , \mathcal{B} , and \mathcal{T} can be analytically computed.

3.2. Recovery Method

We use alternating minimization to solve Equation 10. We first initialize the unknown variables that will be updated in the optimization. Based on experimental exploratory analysis, we set $r_0^{(0)}$ to 0.5. Since \mathcal{A} encodes the absorption of dry surfaces, the initial value $\mathcal{A}^{(0)}$ is set to the spectral observation of the surface subtracted from one (i.e., we use the observed surface color as the initial surface

color). The initial value of the surface absorption coefficient $\mathbf{u}^{(0)}$ can be directly computed from $\mathcal{A}^{(0)}$ and $r_0^{(0)}$. Since the initial value $\mathcal{B}^{(0)}$ will be used to estimate the scattering parameter of a saturated surface g_s , we compute $\mathcal{B}^{(0)}$ using $\gamma_m = 1$, ($m = 1, \dots, M$).

We initialize the gain β using the automatically selected “dry” pixel. If we denote the input spectrum vector for a pixel with W_d , the matrices for that pixel in Equation 8 will be denoted as A_d , B_d , and T_d , whose values are computed using $\mathbf{u}^{(0)}$, $r_0^{(0)}$, g_d and $\gamma = 0$ from Equations 3 and 8. Using W_d , A_d , B_d , and T_d , $\beta^{(0)}$ is initialized by least square optimization

$$\begin{aligned} \beta^{(0)} &= \underset{\beta}{\operatorname{argmin}} \|\beta W_d - (A_d \circ B_d) T_d\|^2 \\ &\text{s.t., } 0 < \beta. \end{aligned} \quad (11)$$

We initialize the scattering parameter for saturated surfaces $g_s^{(0)}$ with constrained nonlinear optimization

$$\begin{aligned} g_s^{(0)} &= \underset{g_s}{\operatorname{argmin}} \|\beta^{(0)} \mathcal{W} - (\mathcal{A}^{(0)} \circ \mathcal{B}^{(0)}) * \mathcal{T}(g_d, g_s, \gamma^{(0)})\|^2 \\ &\text{s.t., } g_d < g_s < 1. \end{aligned} \quad (12)$$

This optimization can be easily solved by using the internal point method since the objective function is a nonlinear function of a scalar g_s with linear constraints.

In the alternating minimization for surface wetness and color recovery, we iteratively optimize the following four sub-problems. Here, we explain the i -th iteration in the optimization. First, we optimize and update the degree of wetness γ using $\mathbf{u}^{(i-1)}$, $r_0^{(i-1)}$, $\beta^{(i-1)}$ and $g_s^{(i-1)}$ by solving

$$\begin{aligned} \gamma^{(i)} &= \underset{\gamma}{\operatorname{argmin}} \|\beta^{(i-1)} \mathcal{W} - (\mathcal{A}^{(i-1)} \circ \mathcal{B}^{(i-1)}) * \mathcal{T}(g_d, g_s^{(i-1)}, \gamma)\|^2 \\ &\text{s.t., } 0 \leq \gamma_m \leq 1 \quad (m = 1, \dots, M). \end{aligned} \quad (13)$$

This optimization can also be easily solved using gradient descent.

Second, we update the multispectral absorption coefficient \mathbf{u} and the mean path length r_0 using $\beta^{(i-1)}$, $\gamma^{(i)}$, and $g_s^{(i-1)}$ by solving

$$\begin{aligned} & \{\mathbf{u}^{(i)}, r_0^{(i)}\} \\ &= \underset{\mathbf{u}, r_0}{\operatorname{argmin}} \|\beta^{(i-1)} \mathcal{W} - (\mathcal{A}(\mathbf{u}, r_0) \circ \mathcal{B}(\mathbf{v}, r_0)) * \mathcal{T}(g_d, g_s^{(i-1)}, \gamma^{(i)})\|^2 \\ & \text{s.t., } 0 \leq u_k \quad (k = 1, \dots, K) \\ & \quad 0 < \gamma_m \leq 1 \quad (m = 1, \dots, M), \end{aligned} \quad (14)$$

where tensors $\mathcal{A}^{(i)}$, $\mathcal{B}^{(i)}$ are updated using the updated parameters $\mathbf{u}^{(i)}$ and $r_0^{(i)}$.

Third, we update the gain $\beta^{(i)}$ using the other variables based on Equation 11. Fourth, we also update the saturated scattering parameter $g_s^{(i)}$ using the other variables based on Equation 12. These four steps are iterated until convergence. After convergence, the final estimates \mathbf{u} , γ , r_0 , g_s are obtained, and tensors \mathcal{A} , \mathcal{B} , and \mathcal{T} can be analytically computed from these estimates.

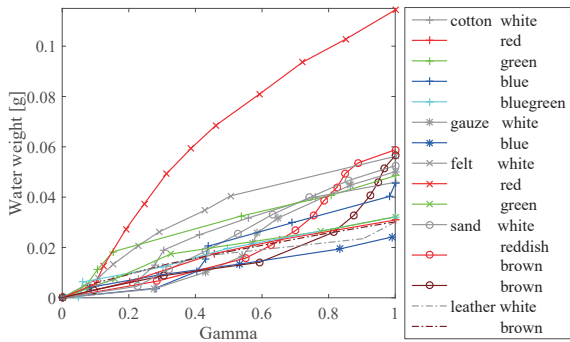


Figure 3: Relation between surface weight and estimated degree of wetness γ during drying of wet cotton, gauze, felt, sand, and leather with several colors, where the horizontal axis is γ , and the vertical axis is weight (g).

	cotton	gauze	felt	sand	leather	all
Ave	0.980	0.977	0.975	0.954	0.980	0.974
Std	0.006	0.024	0.010	0.032	0.002	0.016

Table 1: Correlation coefficients between weight and wetness for each material.

4. Experimental Results

We quantitatively evaluate the accuracy of our model and surface wetness and color recovery method with a comprehensive set of real surfaces. In addition to single colored surfaces, we also demonstrate the application to textured surfaces. In these experiments, we use water as the liquid, but the model and method can be applied to any liquid.

4.1. Surface Wetness

Quantitative evaluation of the estimated degree of wetness, either at a single point or its spatial distribution over a surface, is challenging as there is no simple way to measure the ground truth. To quantitatively evaluate our method’s accuracy with a controlled setup, we assume that the amount of water we dropped on a surface point would be directly proportional to the degree of wetness at that point. This allows us to evaluate the accuracy of the model by comparing the amount of water we drop and the recovered surface wetness. We evaluate this by observing and applying our method to a single surface point.

To generate dry and saturated pixels for a single surface point, which are necessary for our recovery method, we first saturate the surface by dropping a certain amount of water precisely measured with a pipette. Next, the weight of the surface is measured which directly reflects the amount of water absorbed in it, and a multispectral observation is captured with a spectrometer at the surface point. This is iterated several times as the surface dries. The degree of wetness is estimated for each instance using our method.

This experimental process was applied to surfaces with various homogeneous materials (cotton, gauze, felt, sand, and brick) and colors (white, red, green, blue, blue-green,

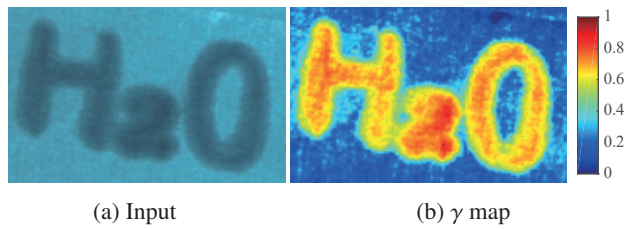


Figure 4: Example of recovered spatial distribution of wetness. Letters “ H_2O ” were drawn on a blue-green cotton surface with water. Our method recovers the surface wetness which clearly captures the spatial distribution corresponding to those letters.

and yellow-green). A wide band white LED was used for illumination, and the incident light was perpendicular to the surface. The illumination and spectrometer were fixed at the same position for all experiments.

Figure 3 shows the relation between the weight (vertical) and the estimated degree of wetness (horizontal). Table 1 shows the average and standard deviation of the correlation coefficient between measured weight and estimated surface wetness γ for each material. In these results, all correlation coefficients take on high values (over 0.95) indicating that the weight and wetness are linearly correlated. This shows that the method accurately estimates the degree of wetness.

4.2. Spatial Distribution of Surface Wetness

Next, we evaluate the recovery accuracy of the spatial distribution of surface wetness. As we cannot measure the ground truth wetness distribution, we qualitatively assess the accuracy. We captured multispectral images with a multispectral camera (EBA Japan NH-8) whose spatial resolution is 1280×1024 pixels and spectral resolution is 5nm in the range from 400nm to 950nm. We used a standard white reference to calibrate the response function of the camera and the spectral distribution of the illumination.

We applied our method to a single multispectral image of a cotton bluegreen surface with the characters “ H_2O ” drawn with water (Figure 4(a)). Figure 4(b) shows the recovered spatial distribution of wetness. We can clearly read the letters in the estimated wetness as the recovered γ map accurately reflects the high contrast degree of wetness induced by the water drawing.

Figure 5 shows detailed results of recovering the parameters of our model from a single multispectral image for a number of real surfaces: green felt, blue felt, red cotton, green cotton, and blue gauze. Figures in column (a) show the input multispectral images visualized in RGB. Figures in (b) show the estimated spatial distributions of surface wetness (i.e., the γ map). We can see that the recovered γ maps agree well with the wetness we see in the input images. These results suggest that our method accurately

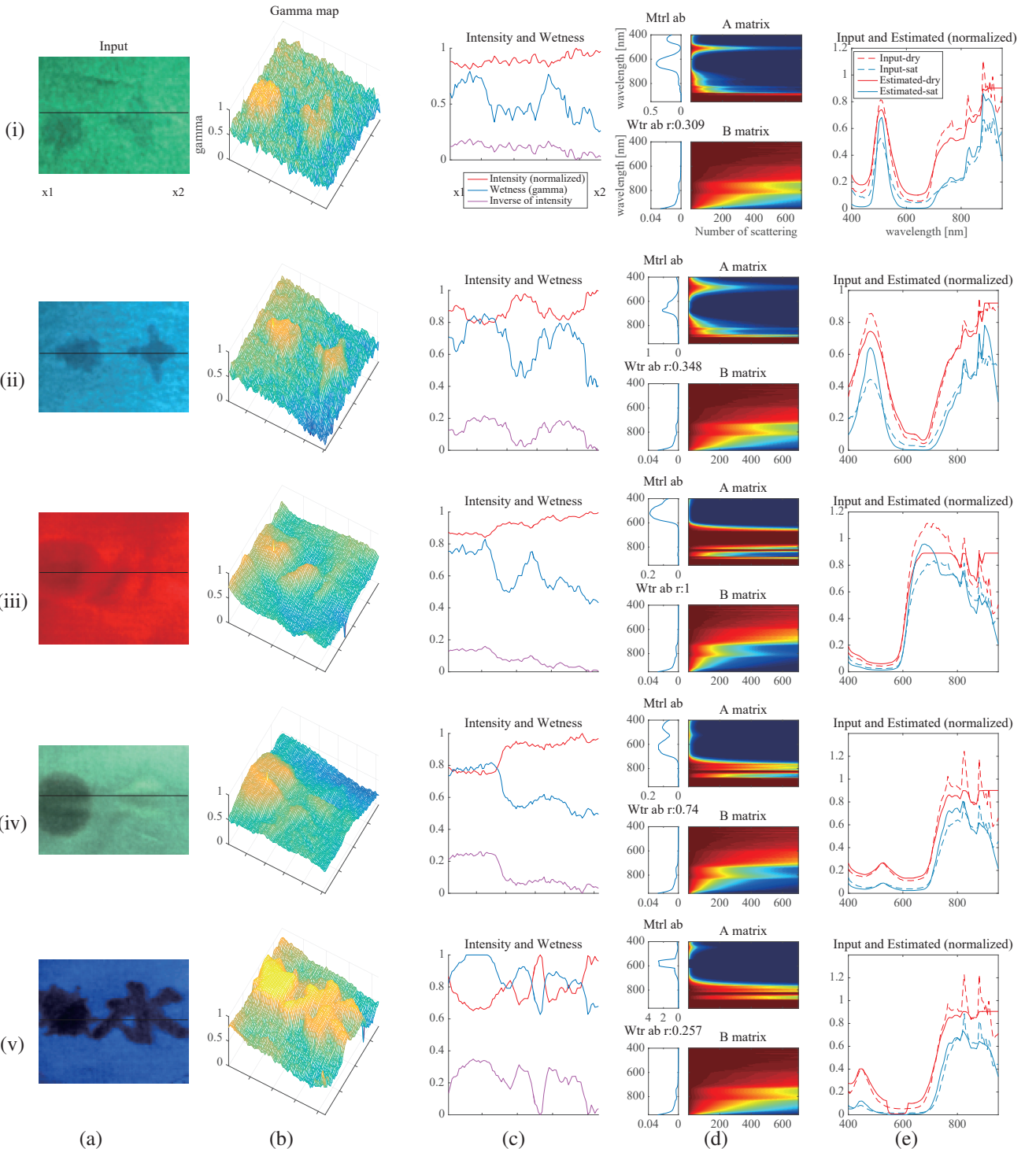


Figure 5: Experimental results of surface wetness and color recovery for various real-world surfaces: felt-green, felt-blue, cotton-red, cotton-green, and gauze-blue. (a) Input image. (b) A 3D γ map showing the spatial distribution of the degree of wetness. (c) Graphs for intensity (red), γ_w (blue) along the black line of (a), and the inverse intensity (magenta). (d) Visualization of recovered dry spectral distribution matrix A (upper) and multiple scattering liquid (water) absorption matrix B (bottom), where the plots on the left show the spectral distributions for single scattering (i.e., first column of the matrices). (e) Comparison of the input multispectral distribution and the recovered distribution using estimated model parameters for dry and saturated surfaces, where the horizontal axis is the wavelength and vertical axis is the magnitude.

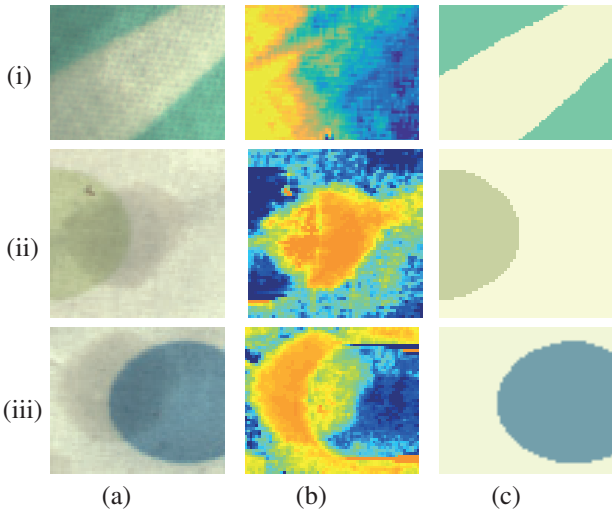


Figure 6: Wetness (b) and surface texture (c) recovered from a single image of wet textured surfaces (a). The recovered spatial wetness and dry texture (albedo) agree well with what we would expect from the input image. The blue area in (iii) is made of material that is more resistant to water.

recovers the surface wetness.

In addition to recovering wetness, our approach can estimate the original surface color (dry spectral distribution) including the absorption and scattering parameters in the optimization. Figure 5(c) shows the distribution of the intensity and the estimated scattering parameter γ_w of surface points taken along the black line in (a), where the horizontal axis indicates spatial x coordinates along the black line, and the vertical axis represents the observed intensity and g . We clearly see that when the intensity increases, g_w decreases. Our results describe the well-known darkening of wet surfaces, and the scattering parameter of dry surfaces is smaller than that of wet surfaces.

Note that the surface wetness is not merely a simple inversion of the observed image intensity. To empirically validate this important point, we plotted the inverse intensity along a cross section shown in the input image for the first surface. As Figure 5(i-c) clearly shows, the surface wetness is indeed different from the inverted input intensity.

Figure 5(d) shows the changes in absorption coefficients of dry surfaces (i.e., matrix A) at the top and those of wet surfaces (i.e., matrix B) at the bottom after multiple scattering. Here the vertical axis represents the sampled wavelengths and the horizontal axis represents the number of scattering n . We also show the first-order absorption coefficients (i.e., single scattering) corresponding to the first column of A and B on the left side of the graphs. In these graphs, we can clearly see that multispectral absorption becomes sharper after multiple scattering. This shows that our model successfully explains the spectral sharpening and contrast increased color of wet surfaces.

Figure 5(e) shows a comparison of the multispectral distribution of dry (blue) and saturated (red) surfaces of the input data (dot line) and its estimated value (solid line) computed as \mathcal{ABT} using the estimated model parameters, where the horizontal axis represents the wavelength and the vertical axis is the intensity observed at each wavelength. Our estimate is very similar to ground truth, which shows that our model can successfully recover the color of dry and saturated surfaces.

4.3. Wet Textured Surfaces

Next, we apply our method to recover the spatial wetness distribution and surface texture (albedo) from a single multispectral image of a wet textured surface. We assume that we can pre-segment the image into single-colored surface regions and apply our model to each region independently. For this, we first classify pixels based on the color using k -means clustering. Since pixels lying on the boundary of different colored regions may not strictly obey our model, we exclude them from the calculation of model parameters. The method is then applied to each colored region separately to recover the spatial wetness and underlying spectral distribution (albedo) and these values are interpolated across the region boundaries.

Figure 6(a) shows input images for several wet textured surfaces. Figure 6(b) shows the estimated spatial distribution of wetness and Figure 6(c) shows the recovered surface texture. In all these results, the wetness maps and surface texture appear to match what we would expect from the input images.

5. Conclusion

In this paper, we derived a spectral appearance model of wet surfaces that explicitly relates the degree of wetness to surface appearance. Our model explains the two fundamental characteristics of wet surface appearance: darkening and spectral sharpening. Based on this model, we introduced a method for recovering the spatial distribution of wetness and the dry color from a single multispectral image of a wet surface. Experimental results using various real-world surfaces validate the accuracy of our model. We believe our model and method provide a sound foundation for leveraging visual cues embedded in wet surfaces and open new avenues of research towards visual analysis of surface conditions.

Acknowledgements This work was supported in part by JSPS KAKENHI Grant Number JP15H05918 to I.S., and the Office of Naval Research grant N00014-16-1-2158 (N00014-14-1-0316) to K.N.

References

- [1] A. Angstrom. The albedo of various surfaces of ground. *Geographic Annals*, 7:323–342, 1925.
- [2] Y. Asano, Y. Zheng, K. Nishino, and I. Sato. Shape from water: Bispectral light absorption for depth recovery. In *Proc. of European Conf on Comp. Vision*, 2016.
- [3] M. Born and E. Wolf. *Principles of Optics*. Pergamon Press, Oxford, 1965.
- [4] H. R. Gordon, O. B. Brown, R. H. Evans, J. W. Brown, R. C. Smith, K. S. Baker, and D. K. Clark. A semianalytic radiance model of ocean color. *Journal of Geophysical Research*, 93(D9):10909–10924, 1988.
- [5] J. Gu, C.-I. Tu, R. Ramamoorthi, P. N. Belhumeur, W. Matusik, and S. K. Nayar. Time-varying surface appearance: Acquisition, modeling and rendering. *ACM Trans. on Graphics*, 25(3):762–771, July 2006.
- [6] A. Ishimaru. *Wave Propagation and Scattering in Random Media*. Academic Press, 1978.
- [7] S. L. Jacques. Optical properties of biological tissues: a review. *Physics in Medicine and Biology*, 58(11), 2013.
- [8] H. W. Jensen, J. Legakis, and J. Dorsey. Rendering of wet materials. In *Rendering Techniques*, pages 273–282, 1999.
- [9] J. Lekner and M. C. Dorf. Why some things are darker when wet. *Applied Optics*, 27(7):1278–1280, 1988.
- [10] J. Lu, A. S. Georgiades, H. Rushmeier, J. Dorsey, and C. Xu. Synthesis of material drying history: Phenomenon modeling, transferring and rendering. In *Eurographics Workshop on Natural Phenomena*, pages 7–16, 2005.
- [11] H. Mall and N. da Vitoria Lobo. Determining wet surfaces from dry. In *IEEE Int'l Conference on Computer Vision*, pages 963–968, 1995.
- [12] Y. Mukaigawa, Y. Yagi, and R. Raskar. Analysis of light transport in scattering media. In *IEEE Conference on Computer Vision and Pattern Recognition 2010*, pages 153–160, 2010.
- [13] J. Stam. Multiple scattering as a diffusion process. In *Eurographics*, pages 41–50, 1995.
- [14] B. Sun, K. Sunkavalli, R. Ramamoorthi, P. N. Belhumeur, and S. K. Nayar. Time-varying brdfs. *IEEE Transactions on Visualization and Computer Graphics*, pages 595–609, May–June 2007.
- [15] V. V. Tuchin. *Selected Papers on Tissue Optics: Applications in Medical Diagnostics and Therapy*. SPIE Milestone Series, 1994.
- [16] S. Twomey, C. Bohren, and J. Mergenthaler. Reflectance and albedo differences between wet and dry surfaces. *Applied Optics*, 25(3):431–437, 1986.
- [17] W. J. Wiscombe and S. G. Warren. A model for the spectral albedo of snow, ii : snow containing atmospheric aerosols. *Journal of the Atmospheric Sciences*, 37:2734–2745, 1980.
- [18] W. J. Wiscombe and S. G. Warren. A model for the spectral albedo of snow, i : pure snow. *Journal of the Atmospheric Sciences*, 37:2712–2733, 1980.
- [19] Y. Yacoob. Matching dry to wet materials. In *IEEE Int'l Conference on Computer Vision*, 2013.
- [20] H. Zhang and K. J. Voss. Bidirectional reflectance study on dry, wet, and submerged particulate layers: effects of pore liquid refractive index and translucent particle concentrations. *Applied Optics*, 45(34):8753–8763, 2006.